Electronic Supplementary Information

Experimental Section

Materials: Ti mesh was provided by Hangxu Filters Flag Store, Hengshui, Hebei. and $K_2B_4O_7 \cdot 4H_2O$, NaOH, $RuCl_3 \cdot 3H_2O$, and $Co(NO_3)_2 \cdot 6H_2O$ were purchased from Aladdin Ltd. (Shanghai, China). Nafion (5 wt%) was purchased from Sigma-Aldrich. All the reagents were used as received. The water used throughout all experiments was purified through a Millipore system.

Preparation of α-$Co(OH)_2$/Ti: Before electrodeposition, Ti mesh was firstly washed with HCl, ethanol, and water several times. The electrodeposition solution contained 0.05 M $Co(NO_3)_2 \cdot 6H_2O$. The deposition was performed in a three-electrode system by a CHI 660E electrochemicalanalyzer (CH Instruments, Inc. Shanghai), using a graphite plate as the counter electrode, Hg/Hg_2Cl_2 (SCE) as the reference electrode, and the cleaned Ti mesh (1×4 cm^2) as the working electrode. The experiment was performed at room temperature (25 C). The electrodeposition of α-$Co(OH)_2$ nanosheets by cyclic voltammetry (CV) was performed within the potential window from -1.2 V to -0.8 V vs. SCE with a scan rate of 50 mV • s^{-1}. After deposition for 50 scan cycles, the as-prepared electrode was rinsed first with deionized water, ethanol for several times and then dried at 60 °C for 12 h in vacuum oven. The sample was annealed at 350 °C in air for 2 h to obtain the Co_3O_4 nanosheets array.

Preparation of Co-Bi/Ti: To obtain Co-Bi/Ti, the α-$Co(OH)_2$/Ti electrode as the working electrode performed by cyclic voltammetry in 0.1 M KBi (pH 9.2) until the current density levelled off, with the graphite plate as the counter electrode and SCE as the reference electrode.

Electrochemical measurements: Electrochemical measurements were performed with a CHI 660E electrochemical analyzer (CH Instruments, Inc., Shanghai) in a conventional three-electrode system. Graphite plate, SCE, and Co-Bi/Ti were used as counter, reference and working electrodes, respectively. Overpotentials (η) were

calculated by the following equation: η = E (RHE) – 1.23 V, where E (RHE) = E (SCE) + (0.242 + 0.059 pH) V. Polarization curves were obtained using linear sweep voltammetry with a scan rate of 2 mVs^{-1} in 0.1M KBi electrolyte. All experiments were carried out at room temperature (298 K).

Characterizations: Powder X-ray powder diffraction (XRD) data of the samples were collected on Bruker D8 ADVANCE Diffractiometer (λ=1.5418 Å).The scanning electron microscopy (SEM) measurements were performed on a XL30 ESEM FEG scanning electron microscope at an accelerating voltage of 20 kV. Transmission electron microscopy (TEM) measurements were performed on a HITACHI H-8100 electron microscopy (Hitachi, Tokyo, Japan) with an accelerating voltage of 200 kV. X-ray photoelectron spectroscopy (XPS) measurements were collected with a Thermal ESCALAB 250 spectrometer using an Al Kα X-ray source (1486.6 eV photons).

Double layer capacitance (C_{dl}) measurements: To measure the electrochemical capacitance, the potential was swept between 1.13 to 1.23 V vs. RHE at different scan rates (60, 80, 100, 120, 140, 160, and 180 mV s^{-1}) with an assumption of double layer charging in the potential range. The capacitive currents at 1.19 V vs. RHE were measured and plotted as a function of scan rate. A linear fit determined the double layer capacitance to be 122 $\mu F\ cm^{-2}$.

Turn over frequency (TOF) calculations: To compare the activity of Co-Bi with other non-noble-metal catalysts, we make a rough estimation of TOF for each active site using the following equation:

$$TOF = JA/4F\ m$$

Where J is current density (A cm^{-2}) at defined overpotential during the LSV measurement in 0.1 M K-Bi; A is the geometric area of the electrode; 4 indicates the mole of electrons consumed for evolving one mole of O_2 from water; F is the Faradic constant (96485 C mol^{-1}); m is the number of active sites (mol), which can be extracted from the linear relationship between the oxidation peak current and scan rate using the following equation:

$$Slope = n^2F^2A\Gamma_0/4RT$$

where n is the number of electrons transferred; F is the Faradic constant; A is the surface area of the electrode; Γ_0 is the surface concentration of active sites (mol cm^{-2}); R and T are the ideal gas constant and the absolute temperature, respectively.

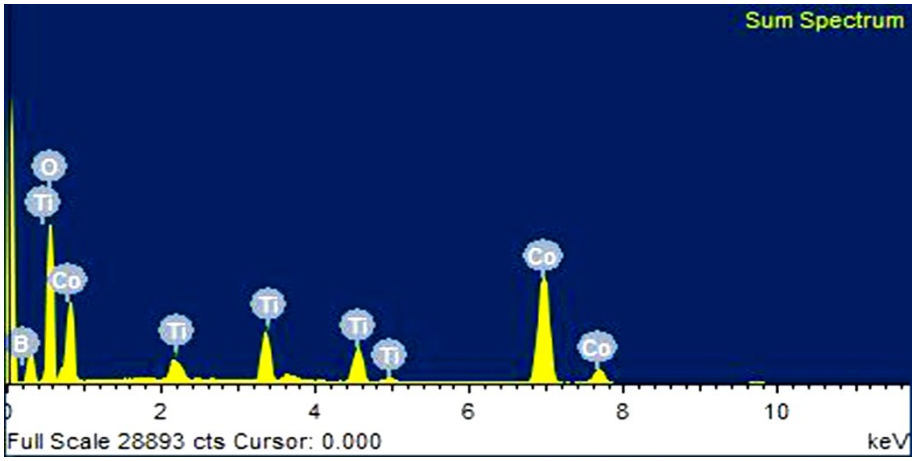

Fig. S1 EDX spectrum of Co-Bi/Ti.

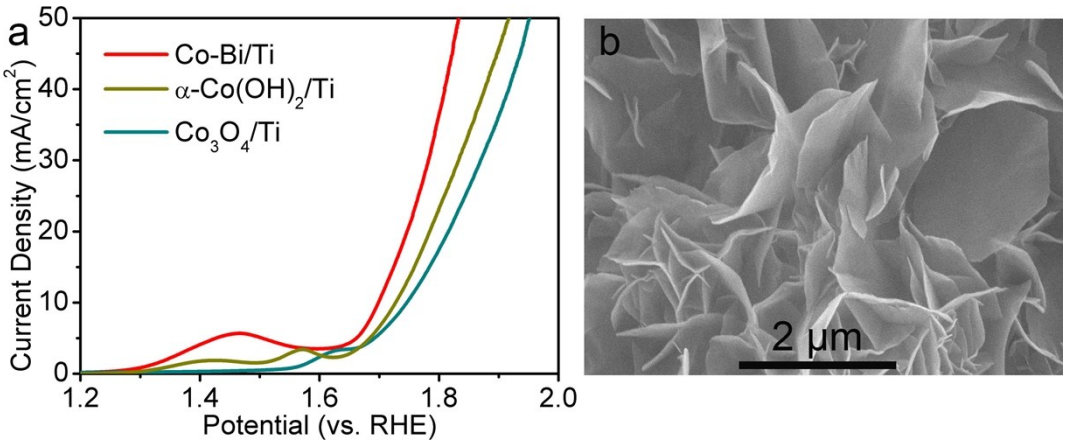

Fig. S2 (a) LSV curves of Co-Bi/Ti, α-$Co(OH)_2$/Ti , and Co_3O_4/Ti for OER in 0.1M KBi. (b) SEM image of Co_3O_4/Ti.

Table S1 Comparison of OER performance for Co-Bi/Ti with other non-noble-metal OER electrocatalysts in neutral or near-neutral media.

Catalyst	j (mA cm^{-2})	η (mV)	Electrolyte	Ref.
Co-Bi/Ti	5	430	0.1 M K-Bi	This work
	10	469	0.1 M K-Bi	
Co-Bi NS/G	10	~490	0.1 M PBS	1
Co-Pi/ITO	1	410	0.1 M PBS	2
Co-Pi/ITO	1	483	0.1 M PBS	3
$Co(PO_3)_2$	10	590	0.1 M PBS	4
$Co(OH)_2$	1	710	0.1 M PBS	5
CoHCF	1	580	0.05 M PBS	6
Co-Bi/FTO	1	390	1 M K-Bi	7
Co_3O_4/SWNTS	5	~700	0.1M PBS	8
Ni-Bi film/ITO	1	~425	0.1 M Bi	9
Ni-Bi film/FTO	0.6	618	0.1 M Na-Bi	10
NiO_x-en/FTO	1	~510	0.6 M Na-Bi	11
NiO_x-Bi	1	~650	0.5 M K-Bi	12
NiO_x-Fe-Bi	5	~552		
Fe-based film/ITO	10	600	0.5 M Na-Bi	13
CuO/FTO	1	~550	0.1 M K-Bi	14
Cu-Bi/FTO	1	~530	0.2 M Na-Bi	15

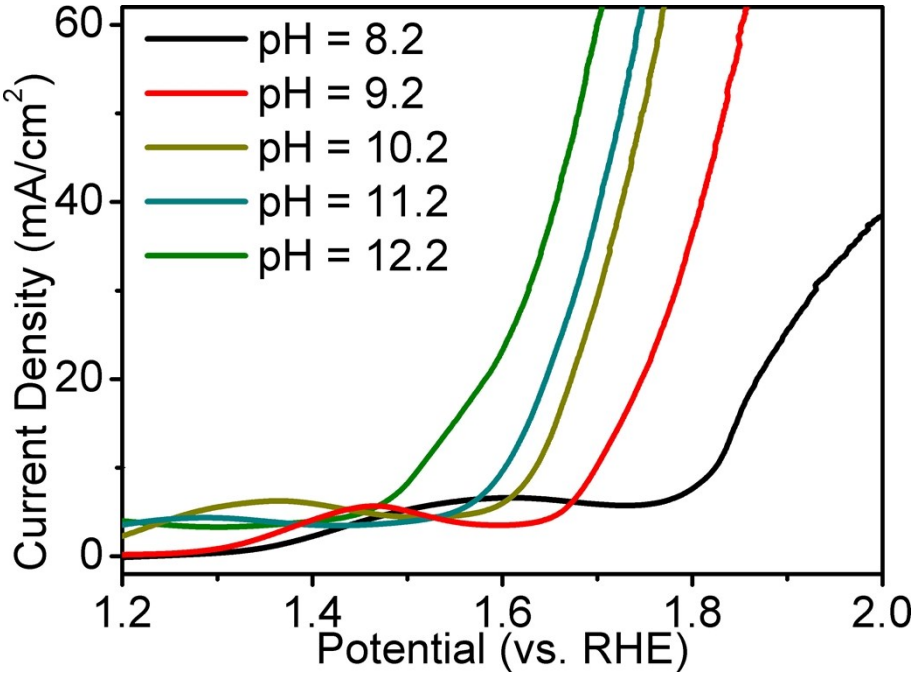

Fig. S3 LSV curves of Co-Bi/Ti for OER in 0.1M K-Bi with different pH.

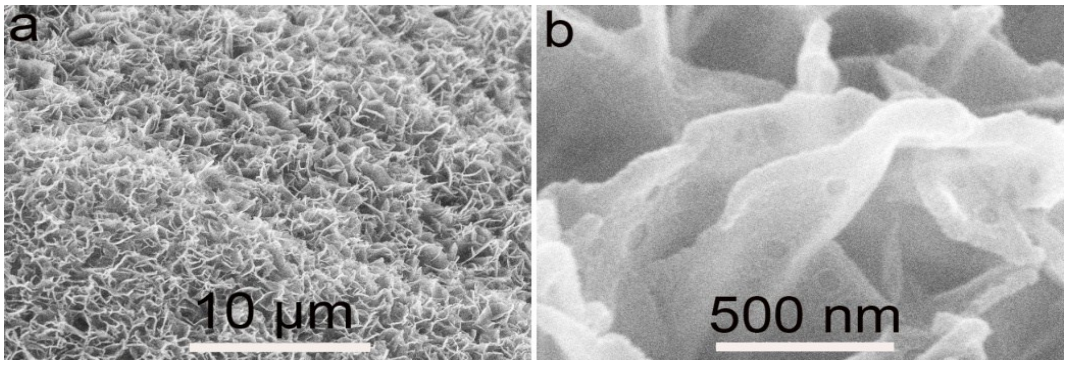

Fig. S4 SEM images of post-OER Co-Bi/Ti.

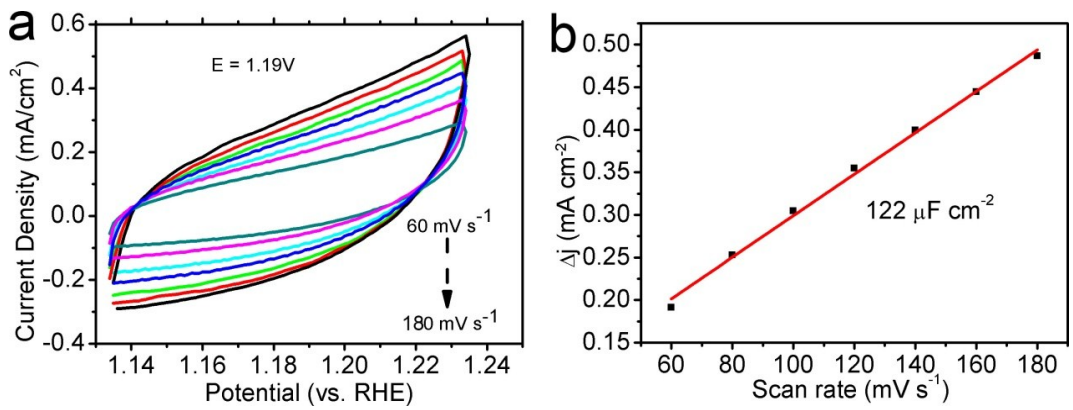

Fig. S5 (a) Cyclic voltammograms for Co-Bi/Ti in the non-faradaic capacitance current range at scan rates of 60, 80, 100, 120, 140, 160, and 180 mV s^{-1}. (b) Capacitive currents for Co-Bi/Ti as a function of scan rate.

References

1 P. Chen, K. Xu, T. Zhou, Y. Tong, J. Wu, H. Cheng, X. Lu, H. Ding, C. Wu and Y. Xie, *Angew. Chem., Int. Ed.*, 2016, **55**, 2488-2492.

2 M. W. Kanan and D. G. Nocera, *Science*, 2008, **312**, 1072-1075.

3 Y. Surendranath, M. Dinca and D. G. Nocera, *J. Am. Chem. Soc.*, 2009, **131**, 2615-2620.

4 H. S. Ahnand and T. D. Tilley, *Adv. Funct. Mater.,* 2013, **23**, 227-233.

5 Y. Zhang, B. Cui, Z. Qin, H. Lin and J. Li, *Nanoscale*, 2013, **5**, 6826-6833.

6 S. Pintado, S. Goberna-Ferron, E. C. Escudero-Adan and J. R. Galán-Mascarós, *J. Am. Chem. Soc.,* 2013, **135**, 13270-13273.

7 A. J. Esswein, Y. Surendranath, S. Y. Reece and D. G. Nocera, *Energy Environ. Sci.,* 2011, **4**, 499-504.

8 J. Wu, Y. Xue, X. Yan, W. Yan, Q. Cheng and Y. Xie, *Nano Res.,* 2012, **5**, 521-530.

9 M. Dincă, Y. Surendranath and D. G. Nocera, *Proc. Natl. Acad. Sci. U.S.A*., 2010, **107**, 10337-10341.

10 C. He, X. Wu and Z. He, *J. Phys. Chem. C.,* 2014, **118**, 4578-4584.

11 A. Singh, S. L. Y. Chang, R. K. Hocking, U. Bach, and L. Spiccia, *Energy Environ. Sci.,* 2013, **6**, 579-586.

12 A. M. Smith, L. Trotochaud, M. S. Burke and S. W. Boettcher, *Chem. Commun.,* 2015, **51**, 5261-5263

13 D. R. Chowdhury, L. Spiccia, S. S. Amritphale, A. Paul and A. Singh, *J. Mater. Chem. A,* 2016, **4**, 3655-3660.

14 X. Liu, S. Cui, Z. Sun and P. Du, *Electrochim. Acta*, 2015, **160**, 202-208.

15 F. Yu, F. Li, B. Zhang, H. Li and L. Sun, *ACS Catal.*, 2015, **5**, 627-630.